Food Research 8 (Suppl. 1) : 36 - 47 (2024)
Journal homepage: https://www.myfoodresearch.com

FOOD RESEARCH

RESEARCH PAPER

Hydrolyzed glucomannan as an encapsulant for various iron concentrations using spray drying method

*Wardhani, D.H., Abdullah, A., Maldini, A., Dyastama, H.K., Ulya, H.N. and Devara, H.R.

Department of Chemical Engineering, Faculty of Engineering, Universitas Diponegoro, Jl. Prof. Sudarto, SH., Tembalang, Semarang 50239, Indonesia

Article history:
Received: 7 March 2023
Received in revised form: 11 October 2023
Accepted: 8 December 2023
Available Online: 3 March 2024

Keywords:
Hydrolyzed glucomannan,
Iron encapsulation,
Spray drying,
Encapsulation properties

DOI:
https://doi.org/10.26656/fr.2017.8(S1).6

Abstract

Among the encapsulation methods, spray-drying is one of the simplest methods to protect iron from oxidation. Hydrolyzed glucomannan (HGM) has shown to have a potential as iron encapsulant in spray drying process due to its ability to form a barrier between the mineral and its surroundings. This work aimed to evaluate the effects of iron concentration (i.e., 20-50 ppm) on the spray dried powder properties using HGM as an encapsulant. The spray drying was conducted using Mini Spray Dryer B-290 Buchi. Feed temperature and aspirator were set at 100°C and 90% aspirator, with 1 mL.min^{-1} of flow rate. Increasing iron did not affect on encapsulation efficiency (98.66-99.4%) but allowed to push loading capacity from 30 to 61.5%. Lower iron concentration tended to result in more uniform particle size of the powders. Iron concentration insignificantly modified crystallinity and functional groups of the powder. Meanwhile, difference in thermal profile of spray-dry powders was observed due to iron concentration.

1. Introduction

Although required in small quantities, iron has important roles for normal growth and is responsible for oxygen absorption, which supports proper human development. Unfulfilled iron consumption at all ages may affect daily activities of humans as it impairs human immunity and stamina (FAO and WHO, 2001). Its deficiency is considered to be the most common cause for all anaemia (Warner and Kamran, 2022), as commonly found in infants and pregnant women. Beside the consumption of iron-rich dietary products, iron supplements and iron-fortified foods help to overcome the iron deficiency problem (Bryszewska, 2019).

Exposed iron is susceptible for oxidation under ambient conditions which influences its aroma, flavor, color and bioavailability (Moslemi *et al.*, 2018). The emergence of these unwanted properties of iron are worse by the presence of inhibitors during food fortification (Bryszewska, 2019). Encapsulation shields the iron and prevents its properties from modification.

Spray-drying encapsulation has advantages compared to other encapsulation methods, such as relative low maintenance cost and stable product (Madene *et al*., 2006). Spray drying produces powder product from the solution of carrier and active agent by droplet atomization in hot air (Jana *et al*., 2017). This method allows the use of various types of carriers as long as it has low viscosity and is able to form droplets during drying. However, the carrier matrix should be chosen considering its food safety and ability to form protection barriers to active agents (Nedovic *et al*., 2011).

Glucomannan had been widely chosen as carrier matrix for various active compounds, such as biological elements and vitamins, as it is able to coat and encapsulate (Yang *et al*., 2009). Furthermore, the drying could strengthen the glucomannan matrix and improve its protection ability (Wattanaprasert *et al*., 2017). However, the viscosity of glucomannan needs to be adjusted so that it can be atomized during the spray drying process. Enzymatic hydrolysis has been reported not only reduce the viscosity but also improve antioxidant activity of hydrolyzed glucomannan (HGM) (Wardhani *et al*., 2022). This antioxidant activity give an additional benefit of HGM as encapsulant on protecting sensitive active compounds from oxidation. Hydrolyzed glucomannan has been reported to encapsulate various active compounds including andrographolide (Wattanaprasert *et al*., 2017) and antitubercular drugs (Guerreiro *et al*., 2019).

Iron encapsulate using spray-drying method has been reported by Churio and Valenzuela (2018) and Romita *et al.* (2011). Churio and Valenzuela (2018) studied the

*Corresponding author.
Email: *dhwardhani@che.undip.ac.id*

eISSN: 2550-2166
Published by Rynnye Lyan Resources

effect of concentrations of bovine erythrocytes and ferrous sulphate using 40% maltodextrin, while Romita *et al.* (2011) used combination of matrixes for ferrous fumarate encapsulation.

Characteristics of a spray drying powder are affected by many factors, including drying-air temperature, carrier type, active compound concentration, and matrix concentrations (Marcela *et al*., 2016; Tchabo *et al*., 2019). Report on the effects of the iron concentration on the spray dry powder properties has been very limited. Hence, this work aimed to evaluate effects of the iron concentration on the spray dry powder properties using HGM as an encapsulant.

2. Materials and methods

2.1 Materials

Glucomannan powder from NOW Foods was used and cellulase powder from *Aspergillus niger* (Sigma Aldrich) with activity ≥0.3 U/mg as raw materials. $FeSO_4.7H_2O$ (Merck KGaA, Darmstadt, Germany) was used as an iron sources. Other chemicals used were in pro analyze grade.

2.2 Iron encapsulation

A thousand milliliter of glucomannan solution (3% w/v) was hydrolyzed by using cellulase (50 $mg.L^{-1}$) under 350 rpm constant stirring at ~28°C. The hydrolysis process was stopped by boiling the solution for 10 min when solution viscosity reached 350 cP. The ferrous sulphate was dissolved in the HGM under constant stirring. Concentration of the ferrous was varied. The mixture was spray-dried using Mini Spray Dryer B-290 Buchi. Feed temperature and aspirator were set at 100°C and 90%, respectively, with 1 $mL.min^{-1}$. Characteristics of HGM-Fe as spray dried powder were determined.

2.3 Iron content, loading capacity and efficiency encapsulation

Iron content of the samples was measured based on Wardhani *et al.* (2022) with slight modification. One gram of sample was dissolved in 50 mL of a sodium citrate solution (100 mM). Ten mL of this solution were mixed with 10 mL a phenanthroline solution (1.0 $g.L^{-1}$), 8.0 mL sodium acetate buffer (98.4 $g.L^{-1}$), and 1.0 mL hydroxylamine hydrochloride solution (100 $g.L^{-1}$) and brought to 100 mL using distilled water. After 10 mins color development, the absorbance of the solution was read at 510 nm against the iron standard.

$$\text{Loading capacity (\%)} = \frac{\text{mass of iron}}{\text{mass of powder sample}} \times 100\%$$

$$\text{Encapsulation efficiency (\%)} = \frac{\text{mass of iron}}{\text{mass of iron added}} \times 100\%$$

2.4 Solubility and swelling

The solubility and swelling of the samples in two pH solutions, i.e., pH 1.2 (HCl, 0.1 M) and pH 6.8 (buffer phosphate, 0.1 M) were determined following the method of Wardhani *et al*. (2022). A hundred milligram of sample was diluted in 10 mL of the pH solution and heated at 60°C. After 30 mins, the sample was centrifuged at 1000 rpm for 10 mins. The supernatant and paste were separated and each was oven-dried after weighed. The solubility and swelling properties were calculated using following equations:

$$\text{Solubility (\%)} = \frac{\text{mass of wet supernatant}}{\text{mass of dried supernatant}} \times 100$$

$$\text{Swelling} = \frac{\text{mass of wet paste}}{\text{mass of dried paste}}$$

2.5 Iron release profile

The concentration of released iron was determined by dispersing the sample (0.1 g) in 50 mL of pH 6.8 solution which was prepared using phosphate buffer, while pH 1.2 was obtained using HCl solution. The samples were placed in orbital shaker. After a certain amount of time, the filtrate was obtained by filtrating the sample and subsequently analyzed for the iron content.

2.6 Particle size distribution

Distribution of particle size was analyzed at 25±1.0◦C for 50 s using a Malvern Panalytical (Malvern, United Kingdom) at a measurement position of 3.00 mm and 8 level of an attenuator. Water was used as the dispersant.

2.7 Morphology and crystallinity

The particle morphology was determined at 20 kV under a magnification of 3000× using scanning electron microscopy (JSM-6510 LV JEOL Ltd., Tokyo, Japan). Meanwhile, the crystallinity of the particles was determined using MAXima_X XRD-7000 diffractometer (Shimadzu, Japan).

2.8 Thermal and functional group analysis

The samples were analyzed for its thermal properties using a Shimadzu DSC-60 Plus differential scanning calorimeter (Shimadzu Corp., Kyoto, Japan). A sample was placed in the alumina crimping cell. The analysis was conducted at temperatures ranging from 30 to 600°C with heating rate of 10°C min^{-1} under an air atmosphere at a flow rate of 10 mL min^{-1}. A Fourier-Transform Infrared Spectroscopy (FTIR) instrument (PerkinElmer Spotlight 200, PerkinElmer Inc., Massachusetts, United States) was used to determined the functional group of the sample.

https://doi.org/10.26656/fr.2017.8(S1).6

3. Results and discussion

In this work, glucomannan which is known as one of the viscous polysaccharides was partially hydrolyzed using cellulase which allowed it to be atomized during spray-drying. It has been reported that ~0.3 Pa.s was the viscosity recommendation for the HGM to be used for spray drying (Wardhani *et al*., 2022). The iron to be encapsulated was varied from 20-50 ppm. For all concentrations, the matrix concentration was set constant at 3%.

3.1 Swelling and solubility

Swelling power is an increase in the volume of a material due to the water absorption process. Solubility is a parameter that measures the ability of the matrix to be dissolved in a system. The two parameters above are important parameters in encapsulation using polymer as the matrix material (Zhang *et al*., 2014). The swelling power of glucomannan-iron particles slightly decreased with the addition of iron concentration (Figure 1). Qiao *et al.* (2017) explained that this decrease in swelling power was caused by the high concentration of iron that covered the surface of glucomannan, thereby inhibiting the process of water absorption by glucomannan particles. Espitia *et al.* (2013) reported that the addition of zinc (Zn) decreased the swelling power of the polymer matrix.

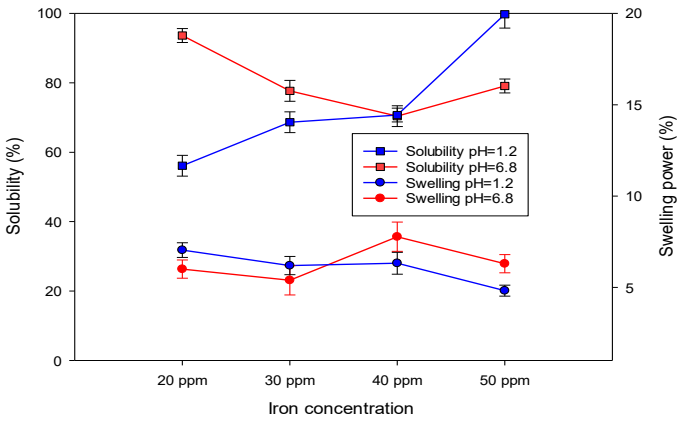

Figure 1. Solubility and swelling power of encapsulated various iron concentrations using hydrolyzed glucomannan in 2 pHs.

At pH 1.2, the solubility of glucomannan-iron particles increased with iron concentration. Iron is very reactive, either in the form of Fe(II) or Fe(III), so it easily binds to the oxygen atom in the hydroxyl group of glucomannan during the encapsulation process (Kumar *et al.,* 2021). During the dissolution process at acidic pH, the glucomannan and iron are released in the presence of hydrogen ions so that more glucomannan-iron powder is dissolved. A similar phenomenon occurred in a study conducted by Saikia *et al.* (2017), where the higher solution of starch-curcumin particles at low pH resulted from the cleavage of hydrogen bond. Ritika *et al*. (2010) argued that swelling power and solubility are influenced by many other factors including to molecular mass, degree of branching, branching chains and contaminant components (Ritika *et al*., 2010). Hence, further study is in needed to find out a synergistic impact of those factors on the swelling power and solubility of the iron particles.

3.2 Iron release

Release of iron was conducted in phosphate buffer at pH 6.8 which denotes the neutrality of human saliva that varies from pH 5.9 to 7.9 (Singh *et al*., 2018). One of the successes in iron encapsulation was indicated by a low iron release during chewing in which the encapsulation was hinder interference in oral cavity. Figure 2 shows release profiles followed diffusion mechanism as the iron has burst release in the first 30 min and continued by an almost steady curve (Farahmandghavi *et al*., 2019). Higher iron concentration was released from the 20 ppm powders than 50 ppm ones. This result supported the solubility result in the previous section, in which the 20 ppm was more soluble than the 50 ppm powders. The maximum iron release was about 30% in 120 mins.

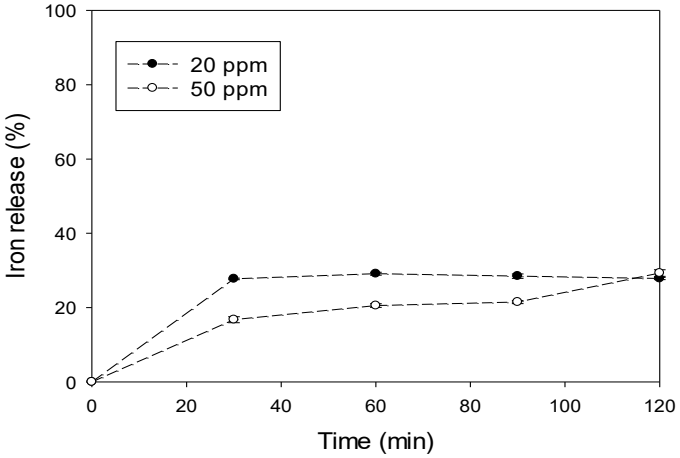

Figure 2. Iron release from encapsulated iron using hydrolyzed glucomannan.

3.3 Loading capacity and encapsulation efficiency

Loading capacity represents the amount of iron per weight of spray dry powders. The loading capacity revealed the capability of the HGM as a matrix to encapsulate iron. Figure 3a shows the positive relation between iron concentration and loading capacity, which range from 30% to 61.5%. Considering the trend, this result suggested that 3% of HGM has potency to entrap higher iron concentration than 50 ppm. This high capability of HGM to trap the iron could be due to its high viscosity though it had been hydrolyzed prior to the drying process. Similar correlation between concentration of active agent and loading capacity was reported by Hou *et al.* (2015) and Wardhani *et al.* (2021). This result was slightly lower than the loading

https://doi.org/10.26656/fr.2017.8(S1).6

reported by Wardhani *et al*. (2021) who use 3% alginate for iron that reached up to 80%, but was superior than Hou *et al.* (2015) who only used the maximum of 12.44% of betaxolol hydrochloride in combination matrix of chitosan-soy protein and Guerreiro *et al.* (2019) who obtained 7.7% of isoniazid in HGM. Meanwhile, there was insignificant EE due to iron concentrations (Figure 3b).

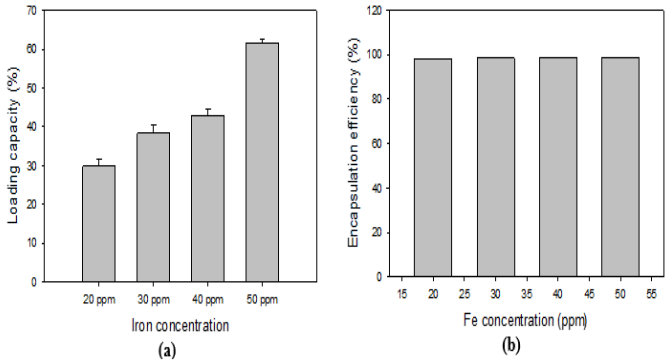

Figure 3. Loading capacity (a) and efficiency encapsulation (b) of encapsulated various iron concentrations using hydrolyzed glucomannan.

3.3 Crystallinity

The XRD result reveals insignificant change of encapsulation powder crystallinity due to iron addition (Figure 4). The samples showed a similar diffraction pattern but difference in peak intensity. The high peaks were found at 19.30, 28.30, 29.24, 32.39, 34.10, 38.84 and 49.01◦ at 2theta. This trend result was corroborated by Wardhani *et al.* (2021) who used hydrolyzed alginate for spray dry matrix of iron. Luo *et al.* (2012) reported that mid-high molecular weight glucomannan over than 2.031×10^4 has amorphous characteristics. However, our XRD profile tended to have higher degree of crystallinity. This could be due to the hydrolysis process of glucomannan prior the spray drying that produced shorter glucomannan chains hence increased the crystallinity. In this work, molecular weight of the glucomannan encapsulant was 1.192×10^4 Da.

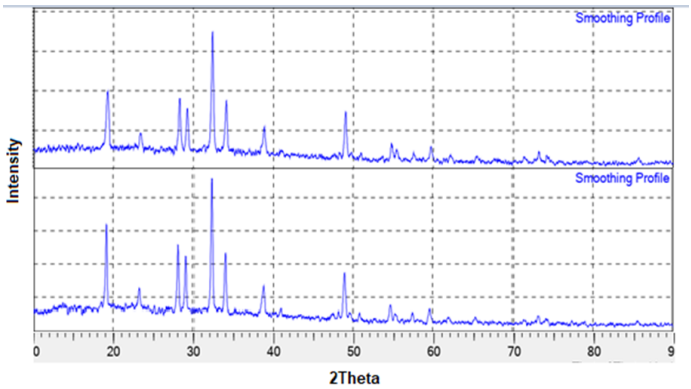

Figure 4. XRD result of encapsulated iron using hydrolyzed glucomannan at iron concentration 20 ppm (top) and 50 ppm (bottom).

3.4 Particle size distribution

The particle size distribution impacted on material properties such as flowability, surface area, conveying properties, extraction and dissolution behavior. Figure 5 shows particle distribution of spray drying powder in different iron concentrations. The average diameter of the 20 ppm powders is 16.635 mm smaller, than that of the 50 ppm powders that is 21.821 mm. Larger particle size was also found by Wardhani *et al.* (2021) by the addition of iron on alginate microparticles. Iron addition increased the total soluble solid, which led the bigger particle formation as found by Dadi *et al.* (2019). However, increasing iron concentration widen the particle size distribution. Particle size of the 20 ppm has a narrower size distribution (10.189-24.199 mm) compared to the range of the 50 ppm powders (0.656-47.466 mm). Iron has different interactions with various polysaccharides types. Several polysaccharides, such as alginate, are easily agglomerated by the presence of iron in solution (Nidhin *et al*., 2008). Similar phenomenon could be occurred in glucomannan solutions. In addition to this variable, other factors could also contribute and interacted synergically to the particle size distribution, including temperature, matrix concentration, matrix type, feed flowrate and atomization (Tontul and Topuz, 2017).

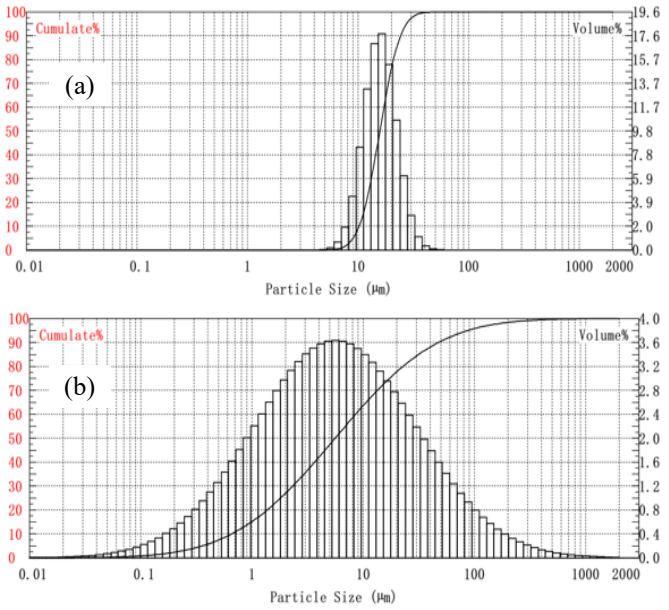

Figure 5. Particle size distribution of encapsulated iron using hydrolyzed glucomannan at iron concentration (a) 20 ppm and (b) 50 ppm.

3.5 Surface morphology

Morphology of particle surface reveals similarity of the powder appearance regardless of the differences in iron contents (Figure 6). Most of the particles have round shape with smooth surface. Only small part of the particles that have a red blood cell shape-like. This result is different with Wardhani *et al.* (2020) who found massive wrinkle of all the encapsulated iron particle

https://doi.org/10.26656/fr.2017.8(S1).6

surface using HGM. This diversity could be due to the difference of spray drying temperature. In this work, the spray drying was conducted at 100°C, lower than Wardhani *et al.* (2020). Lower temperature allowed to have lower rate of moisture diffusion through the encapsulant and created the uniform shrinkage over the particle surface. As a result, the particle was dominated by smooth-surfaced round particles. Moreover, the particle shape is also affected by other factors either the feed properties (e.g., material type, solid concentration, solvent and surfactant) and the drying conditions (e.g., air-inlet temperature) (Arpagaus *et al*., 2017).

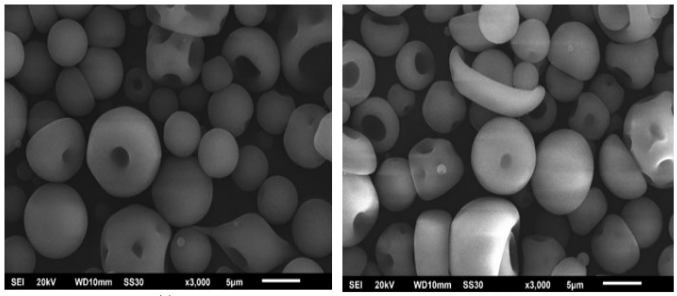

Figure 6. Morphology of encapsulated iron concentrations using hydrolyzed glucomannan of iron concentration (a) 20 ppm and (b) 50 ppm.

3.6 Functional groups and differential scanning calorimetry

Functional groups of the encapsulated iron were detected base on spectroscopy of Fourier-transform infrared between 4000 to 400 cm^{-1}. Overall, additional iron source did not modify any major functional groups. Similar functional groups were found in either the 20 ppm and the 50 ppm sample, but indifference of transmittance level (Figure 7a). All encapsulation samples have the O-H group of wide peak at 3000–3700 cm^{-1} (Wardhani *et al*., 2019), together with the methyl and carbonyl groups, which were assigned to the –CH stretch vibration (~2900 cm^{-1}) and the acetyl groups (1720 cm^{-1}), respectively (Liu *et al*., 2015). A peak of a sulfur from the iron source was found at 1300–1000 cm^{-1}. Increasing concentration of $FeSO_4 \cdot 7H_2O$ as the iron source also led to have bigger peak of O-H group around 3400 cm^{-1} and the peak at 1100 cm^{-1} which belonging to a sulphate group (Gotić and Musić, 2007; Gaihre *et al*., 2008). The peak associated with the hydroxyl group attached to the pyranose rings was identified at ~600 cm-1 (Coates, 2006).

Data of thermal stability of HGM were very important for its application which exposes in high temperature such as in spray dry process. Figure 7b shows the DSC analysis of the encapsulated iron using HGM. Different concentrations of $FeSO_4.7H_2O$ as the iron source led to similar exothermic peaks between 30 - 300°C which has two main peaks, at ~90°C and 320°C. Wang *et al.* (2015) suggested the peak of HGM appeared between 50°C and 130°C which represents to the evaporation of water, while the peak between 280°C and 340°C referred to the main decomposition of molecular chain (Wang *et al*., 2015). Addition of the iron source increased the hydrate contained in the spray dry powders; hence it requires to apply more heat to remove the hydrate. This phenomenon was shown as the enthalpy difference. However, the hydrate in the powders was not completely removed by drying as low drying temperature was applied. To remove all the hydrate, the drying must be conducted at 305°C (Mitchell, 1984). Moreover, Daza *et al.* (2016) found that higher water activity in fruit extract powder decreased the glass transition temperature (Tg). Although more enthalpy was needed to evaporate the water, the Tg of iron powder was slightly increased from 109 to 112°C. This result was contrary with the result of Tan *et al*. (2020) who found that higher moisture content led to lower Tg. Other than the moisture content, the crystallinity of material also influences Tg (Fazaeli *et al*., 2012). The iron addition to the spray-dryer feed might change the crystallinity of spray-dried powder. Decreasing crystallinity was found by Pandey *et al*. (2016) in iron fortification of red rice, as the rice needed to conform itself for iron accommodation. Therefore, further studies are required to confirm the effect of iron addition on thermal properties of material.

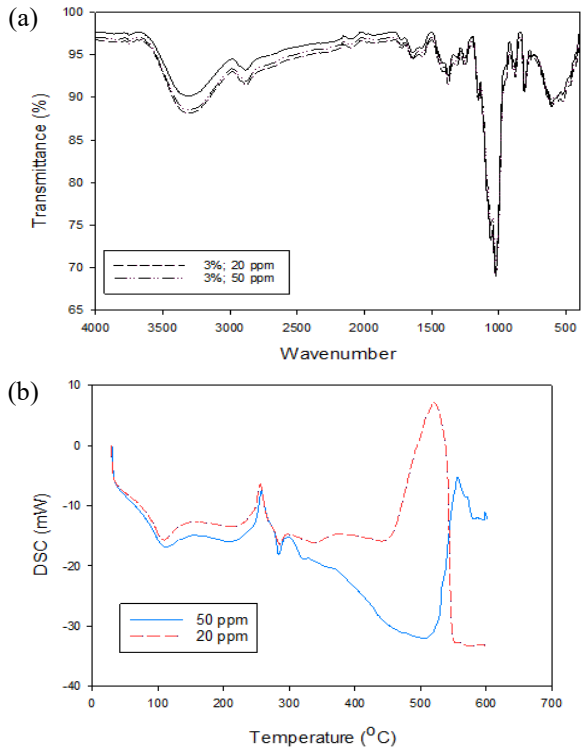

Figure 7. (a) Functional groups and (b) DSC result of encapsulated iron using hydrolyzed glucomannan.

https://doi.org/10.26656/fr.2017.8(S1).6

4. Conclusion

The effectiveness of encapsulation is not only affected by the matrix type, but also the core concentration. Iron, as the core, can be maximally entrapped in glucomannan powder by increasing the iron concentration in spray-dryer's feed. However, faster release was occurred at lower iron concentration powders. The iron concentration difference did not change the functional group of spray-dried iron powder and insignificantly increases the powder crystallinity. Profile of the thermal properties of the iron powders varied with iron concentration.

Conflict of interest

The authors declare no conflict of interest.

Acknowledgments

The authors acknowledge the Faculty of Engineering, Universitas Diponegoro-Indonesia through Strategic Research Grant 2022 scheme, for funding the research.

References

Arpagaus, C., John, P., Collenberg, A. and Rütti, D. (2017). Nanocapsules formation by nano spray drying. In Jafari, S.M. (Ed.). Nanoencapsulation Technologies for the Food and Nutraceutical Industries, p. 345-501. Cambridge, United Kingdom: Academic Press. https://doi.org/10.1016/B978-0-12-809436-5.00010-0

Bryszewska, M.A. (2019). Comparison study of iron bioaccessibility from dietary supplements and microencapsulated preparations. *Nutrients,* 11(2), 273. https://doi.org/10.3390/nu11020273

Churio, O. and Valenzuela, C. (2018). Development and characterization of maltodextrin microparticles to encapsulate heme and non-heme iron. *LWT-Food Science and Technology,* 96, 568-575. https://doi.org/10.1016/j.lwt.2018.05.072

Coates, J. (2006). Interpretation of Infrared Spectra, A Practical Approach. In Meyer, R.A. (Ed.). Encyclopedia of Analytical Chemistry, p. 10881–10882. Larkspur, USA: RAMTECH, Inc

Dadi, D.W., Emire, S.A., Hagos, A.D. and Eun, J.B. (2019). Effects of spray drying process parameters on the physical properties and digestibility of the microencapsulated product from Moringa stenopetala leaves extract. *Cogent Food and Agriculture*, 5(1), 1690316. https://doi.org/10.1080/23311932.2019.1690316

Daza, L.D., Fujita, A., Fávaro-Trindade, C.S., Rodrigues -Ract, J.N., Granato, D. and Genovese, M.I. (2016). Effect of spray drying conditions on the physical properties of Cagaita (*Eugenia dysenterica* DC.) fruit extracts. *Food and Bioproducts Processing*, 97, 20-29. https://doi.org/10.1016/j.fbp.2015.10.001

Espitia, P.J.P., Soares, N.D.F.F., Teófilo, R.F., dos Reis Coimbra, J.S., Vitor, D.M., Batista, R.A., Ferreira, S.O., de Andrade, N.J. and Medeiros, E.A.A. (2013). Physical-mechanical and antimicrobial properties of nanocomposite films with pediocin and ZnO nanoparticles. *Carbohydrate Polymer*, 94, 199-208. https://doi.org/10.1016/j.carbpol.2013.01.003

FAO and WHO. (2001). Human vitamin and mineral requirements. Report of a joint FAO/WHO expert consultation. Rome, Italy: Food and Nutrition Division FAO Rome

Farahmandghavi, F., Imani, M. and Hajiesmaeelian, F. (2019). Silicone matrices loaded with levonorgestrel particles: Impact of the particle size on drug release. *Journal of Drug Delivery Science and Technology,* 49, 132–142. https://doi.org/10.1016/j.jddst.2018.10.029

Fazaeli, M., Emam-Djomeh, Z., Kalbasi Ashtari, A. and Omid, M. (2012). Effect of spray drying conditions and feed composition on the physical properties of black mulberry juice powder. *Food and Bioproducts Processing,* 90(4), 667-675. https://doi.org/10.1016/j.fbp.2012.04.006

Gaihre, B., Aryal, S., Barakat, N.A.M. and Kim, H.Y. (2008). Gelatin stabilized iron oxide nanoparticles as a three dimensional template for the hydroxyapatite crystal nucleation and growth. *Materials Science and Engineering C,* 28(8), 1297-1303. https://doi.org/10.1016/j.msec.2008.01.001

Gotić, M. and Musić, S. (2007). Mössbauer, FT-IR and FE SEM investigation of iron oxides precipitated from $FeSO_4$ solutions. *Journal of Molecular Structure,* 834–836, 445-453. https://doi.org/10.1016/j.molstruc.2006.10.059

Guerreiro, F., Pontes, J.F., Rosa da Costa, A.M. and Grenha, A. (2019). Spray-drying of konjac glucomannan to produce microparticles for an application as antitubercular drug carriers. *Powder Technology,* 342, 246–252. https://doi.org/10.1016/j.powtec.2018.09.068

Hou, D., Gui, R., Hu,S., Huang, Y., Feng, Z. and Ping, Q. (2015). Preparation and characterization of novel drug-inserted-montmorillonite chitosan carriers for ocular drug delivery. *Advances in Nanoparticles*, 4 (3), 70-84. https://doi.org/10.4236/anp.2015.43009

Jana, S., Gandhi, A. and Jana, S. (2017). Nanotechnology in Bioactive Food Ingredients: Its

Pharmaceutical and Biomedical Approaches. In Oprea, A.E. and Grumezescu, A.M. (Eds.). Nanotechnology Applications in Food: Flavor, Stability, Nutrition and Safety. Cambridge, United Kingdom: Academic Press. https://doi.org/10.1016/B978-0-12-811942-6.00002-9

Kumar, S., Madan, S., Bariha, N. and Suresh, S. (2021). Swelling and shrinking behavior of modified starch biopolymer with iron oxide. *Starch - Stärke*, 73(3-4), 2000108. https://doi.org/10.1002/star.202000108

Liu, J., Xu, Q., Zhang, J., Zhou, X., Lyu, F., Zhao, P. and Ding, Y. (2015). Preparation, composition analysis and antioxidant activities of konjac oligo-glucomannan. *Carbohydrate Polymers*, 130, 398–404. https://doi.org/10.1016/j.carbpol.2015.05.025

Luo, X., Yao, X., Zhang, C., Lin, X. and Han, B. (2012). Preparation of mid-to-high molecular weight konjac glucomannan (MHKGM) using controllable enzyme -catalyzed degradation and investigation of MHKGM properties. *Journal of Polymer Research*, 19(4), 9849. https://doi.org/10.1007/s10965-012-9849-x

Madene, A., Jacquot, M., Scher, J. and Desobry, S. (2006). Flavour encapsulation and controlled release - A review. *International Journal of Food Science and Technology*, 41(1), 1–21. https://doi.org/10.1111/j.1365-2621.2005.00980.x

Marcela, F., Lucía, C., Esther, F. and Elena, M. (2016). Microencapsulation of l-ascorbic acid by spray drying using sodium alginate as wall material. *Journal of Encapsulation and Adsorption Sciences*, 06(01), 1–8. https://doi.org/10.4236/jeas.2016.61001

Mitchell, A.G. (1984). The preparation and characterization of ferrous sulphate hydrates. *Journal of Pharmacy and Pharmacology,* 36(8), 506 -510. https://doi.org/10.1111/j.2042-7158.1984.tb04440.x

Moslemi, M., Hosseini, H., Neyestani, T.R., Akramzadeh, N. and Fard, M.N.R. (2018). Effects of non-digestive polymers used in iron encapsulation on calcium and iron apparent absorption in rats fed by infant formula. *Journal of Trace Elements in Medicine and Biology*, 50, 393-398. https://doi.org/10.1016/j.jtemb.2018.08.004

Nedovic, V., Kalusevic, A., Manojlovic, V., Levic, S. and Bugarski, B. (2011). An overview of encapsulation technologies for food applications. *Procedia Food Science*, 1, 1806–1815. https://doi.org/10.1016/j.profoo.2011.09.265

Nidhin, M., Indumathy, R., Sreeram, K.J. and Nair, B.U. (2008). Synthesis of iron oxide nanoparticles of narrow size distribution on polysaccharide templates. *Bulletin of Materials Science,* 31(1), 93-96. https://doi.org/10.1007/s12034-008-0016-2

Pandey, S., Asha, M.R. and Jayadep, A. (2016). Changes in physical, cooking, textural properties and crystallinity upon iron fortification of red rice (Jyothi). *Journal of Food Science and Technology*, 53(2), 1014-1024. https://doi.org/10.1007/s13197-015-2130-7

Qiao, D., Yu, L., Bao, X., Zhang, B. and Jiang, F. (2017). Understanding the microstructure and absorption rate of starch-based superabsorbent polymers prepared under high starch concentration. *Carbohydrate Polymers*, 175, 141-148. https://doi.org/10.1016/j.carbpol.2017.07.071

Ritika, B.Y., Khatkar, B.S. and Baljeet, S.Y. (2010) Physicochemical, Morphological, Thermal and Pasting Properties of Starches Isolated from Rice Cultivars Grown in India. *International Journal of Food Properties,* 13(6), 1339-1354. https://doi.org/10.1080/10942910903131407

Romita, D., Cheng, Y.L. and Diosady, L.L. (2011). Microencapsulation of ferrous fumarate for the production of salt double fortified with iron and iodine. *International Journal of Food Engineering*, 7, 3. https://doi.org/10.2202/1556-3758.2122

Saikia, C., Das, M.K., Ramteke, A. and Maji, T.K. (2017). Evaluation of folic acid tagged aminated starch/ZnO coated iron oxide nanoparticles as targeted curcumin delivery system. *Carbohydrate Polymers,* 157, 391-399. https://doi.org/10.1016/j.carbpol.2016.09.087

Singh, P.A., Siddiqui, J. and Diosady, L.L. (2018). Characterizing the pH-dependent release kinetics of food-grade spray drying encapsulated iron microcapsules for food fortification. *Food and Bioprocess Technology,* 11(2), 435-446. https://doi.org/10.1007/s11947-017-2022-0

Tan, S., Zhong, C. and Langrish, T. (2020). Encapsulation of caffeine in spray-dried micro-eggs for controlled release: The effect of spray-drying (cooking) temperature. *Food Hydrocolloids*, 108, 105979. https://doi.org/10.1016/j.foodhyd.2020.105979

Tchabo, W., Ma, Y., Kaptso, G.K., Kwaw, E., Cheno, R.W., Xiao, L., Osae, R., Wu, M. and Farooq, M. (2019). Process analysis of mulberry *(Morus alba)* leaf extract encapsulation: effects of spray drying conditions on bioactive encapsulated powder quality. *Food and Bioprocess Technology,* 12(1), 122–146. https://doi.org/10.1007/s11947-018-2194-2

Tontul, I. and Topuz, A. (2017). Spray-drying of fruit and vegetable juices: Effect of drying conditions on

the product yield and physical properties. *Trends in Food Science and Technology*, 63, 91-102. https://doi.org/10.1016/j.tifs.2017.03.009

Wang, S., Zhou, B., Wang, Y. and Li, B. (2015). Preparation and characterization of konjac glucomannan microcrystals through acid hydrolysis. *Food Research International*, 67, 111–116. https://doi.org/10.1016/j.foodres.2014.11.008

Wardhani, D.H., Cahyono, H., Ulya, H.N., Kumoro, A.C., Anam, K. and Vázquez, J.A. (2022). Spray-dryer feed preparation: Enzymatic degradation of glucomannan for iron nanoencapsulation. *AIMS Agriculture and Food,* 7(3), 683–703. https://doi.org/10.3934/agrfood.2022042

Wardhani, D.H., Ulya, H.N., Rahmawati, A., Sugiarto, T.V.K., Kumoro, A.C. and Aryanti, N. (2021). Preparation of degraded alginate as a pH-dependent release matrix for spray-dried iron and its encapsulation performances. *Food Bioscience*, 41, 101002. https://doi.org/10.1016/j.fbio.2021.101002

Wardhani, D.H., Vázquez, J.A., Ramdani, D.A., Lutfiati, A., Aryanti, N. and Cahyono, H. (2019). Enzymatic purification of glucomannan from *Amorphophallus oncophyllus* using A-amylase. *Bioscience Journal*, 35(1), 277–288. https://doi.org/10.14393/BJ-v35n1a2019-41766

Wardhani, D.H., Wardana, I.N., Ulya, H.N., Cahyono, H., Kumoro, A.C. and Aryanti, N. (2020). The effect of spray-drying inlet conditions on iron encapsulation using hydrolyzed glucomannan as a matrix. *Food and Bioproducts Processing*, 123, 72–79. https://doi.org/10.1016/j.fbp.2020.05.013

Warner, M.J. and Kamran, M.T. (2022). Iron Deficiency Anemia. StatPearls E-Book. Retrieved from NCBI website: https://www.ncbi.nlm.nih.gov/books/NBK448065/.

Wattanaprasert, S., Borompichaichartkul, C., Vaithanomsat, P. and Srzednicki, G. (2017). Konjac glucomannan hydrolysate: A potential natural coating material for bioactive compounds in spray drying encapsulation. *Engineering in Life Sciences,* 17(2), 145–152. https://doi.org/10.1002/elsc.201600016

Yang, J., Xiao, J.X. and Ding, L.Z. (2009). An investigation into the application of konjac glucomannan as a flavor encapsulant. *European Food Research and Technology*, 229(3), 467–474. https://doi.org/10.1007/s00217-009-1084-2

Zhang, C., Chen, J. and Yang, F.-Q. (2014). Konjac glucomannan, a promising polysaccharide for OCDDS. *Carbohydrate Polymers*, 104, 175–181.https://doi.org/10.1016/j.carbpol.2013.12.081

